ORGANOMETALLICS

Article

Cite This: *Organometallics* 2019, 38, 4250−4260

pubs.acs.org/Organometallics

Olefin Insertion Reactivity of a (Phosphine-arenesulfonate)Palladium(II) Fluoride Complex

Rebecca E. Black,[†] Stefan M. Kilyanek,[‡] Erik D. Reinhart,[§] and Richard F. Jordan*[,§]

[†]Department of Chemistry, New College of Florida, 5800 Bay Shore Road, Sarasota, Florida 34243, United States

[‡]Department of Chemistry & Biochemistry, University of Arkansas, 119 Chemistry Building, Fayetteville, Arkansas 72701, United States

[§]Department of Chemistry, The University of Chicago, 5735 South Ellis Avenue, Chicago, Illinois 60637, United States

Supporting Information

ABSTRACT: The synthesis of the phosphine-arenesulfonate Pd(II) fluoride complex (PO-OMe)PdF(lut) (**2**, PO-OMe = P(2-OMe-Ph)$_2$(2-SO$_3$-5-Me-Ph), lut = 2,6-lutidine) and its reactions with electron-deficient olefins are described. The reaction of (PO-OMe)PdBr(lut) (**1**) with AgF affords **2** as an 82:18 mixture of *cis-P,F* and *trans-P,F* isomers. **2** isomerizes to a 1:2 *cis-P,F*:*trans-P,F* equilibrium mixture in CD_2Cl_2 solution at room temperature in ca. 3 days. **2** reacts with vinyl fluoride (VF) to afford (PO-OMe)Pd(CH_2CHF_2)(lut) (**3**), which exists as the *cis-P,C* isomer. **2** reacts with vinyl bromide (VBr) to yield **1** and VF by initial fluoropalladation to form (PO-OMe)Pd(CH_2CHBrF)(lut) (**4**, not observed) followed by *β*-Br elimination. **2** reacts with vinyl acetate to yield (PO-OMe)Pd{$CH_2CHF(OAc)$}(lut) (**5**), which reacts further to form the C-bound enolate complex (PO-OMe)Pd{$CH_2C(=O)H$}(lut) (**6**) and acetyl fluoride. **2** reacts with vinyl benzoate in an analogous fashion. DFT analysis of the reaction of the model complexes *cis-P,F-* and *trans-P,F*-(PH_2O)PdF(py) (**C1** and **C2**, PH_2O^- = *o*-$PH_2C_6H_4SO_3^-$) with VF supports a mechanism involving substitution of lutidine by VF followed by migratory insertion into the Pd−F bond. An alternative mechanism comprising substitution of fluoride by VF to generate (PO-OMe)Pd(VF)(lut)$^+$ and F^-, followed by exo attack of F^- on the bound VF was found to be energetically prohibitive. DFT analysis of the reaction of the model complexes *cis-P,F-* and *trans-P,F*-(PH_2O)PdF(VBr) (**C10** and **C13**) supports an insertion/*β*-Br elimination mechanism.

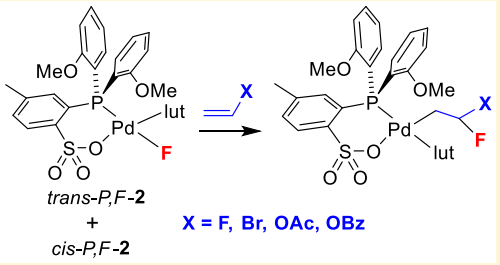

INTRODUCTION

The insertion of olefins and alkynes into metal-fluoride bonds generates new M−C and C−F bonds and therefore is of interest for the synthesis of fluorinated organic compounds and polymers.[1] Alkali metal fluorides, AgF and HgF_2 undergo fluorometalation reactions with highly fluorinated olefins and alkynes to afford fluorinated alkyl and alkenyl species that have been exploited in synthesis, but analogous reactions of unactivated substrates are rare.[2,3] (SIPr)AuF reacts with internal alkynes to yield *trans* addition products via nucleophilic attack of F^- on an intermediate Au alkyne complex.[4] Insertions of styrenes and alkynes into Pd−F bonds were proposed as key steps in the Pd-catalyzed amino-fluorination and fluoroesterification of styrenes and fluorination/cyclization of enynes.[5] Wada and Jordan recently reported that the discrete Pd−F complex ($PO^{Bp,OMe}$)PdF(lut) (**A**, $PO^{Bp,OMe}$ = P(2-OMe-Ph){2′,6′-$(OMe)_2$-2-biphenyl}(2-SO_3-5-Me-Ph), lut = 2,6-lutidine) undergoes 1,2 insertion of vinyl fluoride (VF) at room temperature to generate ($PO^{Bp,OMe}$)-Pd(CH_2CHF_2)(lut) (**B**, Scheme 1).[6] Complexes **A** and **B** undergo repetitive ethylene insertions at room temperature to produce polyethylenes with $-CH_2CH_2F$ and $-CH_2CHF_2$ chain end units, respectively. These reactions play an important role in the copolymerization of ethylene and VF catalyzed by ($PO^{Bp,OMe}$)PdMe(lut) and other (phosphine-arenesulfonate)PdRL complexes, as they reactivate the Pd−F species that are generated by *β*-F elimination of $PdCH_2CHRF$ species.[7] In contrast, in other attempted ethylene/vinyl-halide

Scheme 1. Reaction of ($PO^{Bp,OMe}$)PdF(lut) with Vinyl Fluoride and Ethylene[6]

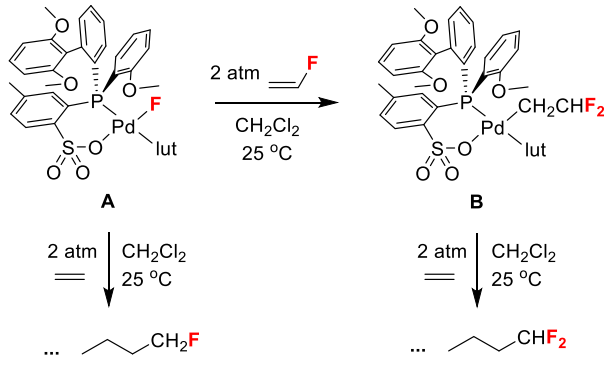

Received: August 9, 2019
Published: October 15, 2019

DOI: 10.1021/acs.organomet.9b00545
Organometallics 2019, 38, 4250−4260

copolymerizations, β-halide elimination produces inactive L_nMX species and thus is a catalyst deactivation process.[8,9]

The objective of this paper is to expand the range of known (PO)Pd fluoride complexes and to probe the generality of their reactions with olefins. We report the synthesis of a new Pd−F complex, (PO-OMe)PdF(lut) (**2**), which contains the prototypical phosphine-arenesulfonate ligand P(2-OMe-Ph)$_2$(2-SO$_3$-5-Me-Ph) (PO-OMe). Insertion reactions of **2** with VF, vinyl bromide (VBr), vinyl acetate (VOAc), and vinyl benzoate (VOBz), and a DFT computational analysis of the VF and VBr reactions are discussed.

RESULTS AND DISCUSSION

Synthesis and Characterization of (PO-OMe)PdF(lut). The target compound (PO-OMe)PdF(lut) (**2**) was synthesized by the reaction of the corresponding bromide complex (PO-OMe)PdBr(lut) (**1**) with AgF (Scheme 2), following the approach used to prepare **A** and other Pd−F complexes.[10] The reaction of the zwitterionic pro-ligand HP$^+$(2-OMe-Ph)$_2$(2-SO$_3^-$-5-Me-Ph) with (COD)PdBr$_2$ followed by addition of lutidine yielded **1** and lutidinium bromide, the latter of which was removed by a water wash. **1** was isolated as orange crystals in 77% yield by recrystallization from CH_2Cl_2/pentane and characterized by X-ray diffraction (Figure 1). Complex **1** adopts a *cis-P,Br* structure with metrical parameters similar to those for (PO^{Bp,OMe})PdBr(lut).[6] The reaction of **1** with AgF in CH_2Cl_2 afforded **2** as an 82:18 mixture of *cis-P,F* and *trans-P,F* isomers (95%, Scheme 2).

Scheme 2. Synthesis of (PO-OMe)PdF(lut)

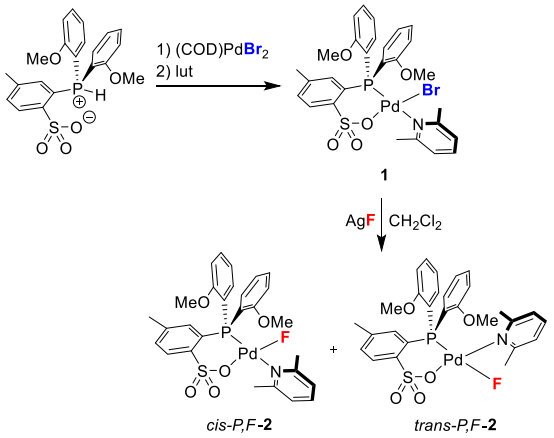

Complex **2** isomerizes to a 1:2 *cis-P,F*:*trans-P,F* equilibrium mixture in CD_2Cl_2 solution at room temperature in ca. 3 d. **2** also isomerizes slowly (months) in the solid state. Previous studies have shown that an external ligand is necessary for the *cis*/*trans* isomerization of (PO-OMe)PdCl{P(*o*-tolyl)$_3$} and that *trans-P,C*-(PO-OMe)PdMeL complexes (L = lut or *para*-substituted lutidines) isomerize to the thermodynamically favored *cis-P,C* isomer by both lutidine-catalyzed and unimolecular pathways.[11] On the basis of these precedents, both ligand-catalyzed and unimolecular pathways are possible for the *cis*/*trans* isomerization of **2**. The isomerization behavior of **2** stands in contrast to the behavior of **A**, for which only the *cis-P,F* isomer was observed.[6] *trans-P,F*-(PO^{Bp,OMe})PdF(lut) is likely disfavored by steric crowding between the PO^{Bp,OMe} and lutidine ligands.

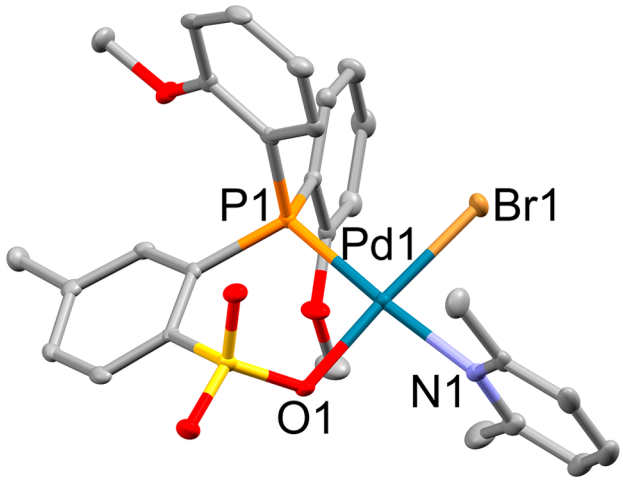

Figure 1. Molecular structure of **1**·CH_2Cl_2. Hydrogen atoms and the CH_2Cl_2 solvent molecule are omitted for clarity. Key bond lengths (Å) and angles (deg): Pd1−Br1 2.3903(4), Pd1−N1 2.113(3), Pd1−O1 2.069(2), Pd1−P1 2.2483(9), Br1−Pd1−N1 88.26(7), N1−Pd1−O1 87.84(9), Br1−Pd1−P1 88.40(2), O1−Pd1−P1 95.51(6).

The room temperature $^{31}P\{^1H\}$ NMR spectrum of **2** in the presence of added CsF (vide infra), contains two doublets at δ 3.0 ($^2J_{PF}$ = 210 Hz) and δ −4.7 ($^2J_{PF}$ = 16 Hz), which are assigned to the *trans-P,F* and *cis-P,F* isomers, respectively. The room temperature ^{19}F NMR spectrum contains a doublet at δ −267 ($^2J_{PF}$ = 210) and a broad singlet at δ −436, which sharpens into a doublet ($^2J_{PF}$ = 16) at −15 °C, which are assigned to the *trans-P,F* and *cis-P,F* isomers, respectively. These data are consistent with data for other Pd(II) fluoride complexes bearing phosphine ligands *trans* to fluoride (^{19}F δ −200 to −300; $^2J_{PF,trans}$ > 150 Hz) and *cis* to fluoride (^{19}F δ < −300; $^2J_{PF,cis}$= 6−18 Hz).[1−8,12] The addition of excess [NBu$_4$]Br to *cis*:*trans-P,F*-**2** (32:68 ratio) gives **1** quantitatively, which confirms that these species are isomers.

The addition of CsF was required to observe all of the ^{31}P and ^{19}F NMR couplings for *cis-P,F*- and *trans-P,F*-**2**. In the absence of CsF in dry CD_2Cl_2, the P−F coupling is observed for the ^{31}P resonance of *cis-P,F*-**2**, but not for the ^{31}P resonance of *trans-P,F*-**2** or the ^{19}F resonances of either isomer. The collapse of the P−F coupling is ascribed to hydrogen bonding with adventitious water or HF. CsF sequesters adventitious water through hydrogen bonding.[10j,13] Intermolecular fluoride exchange is unlikely because P−F coupling would not be observed for the ^{31}P resonance of *cis-P,F*-**2** in this case.

Reaction of 2 with Vinyl Fluoride. Compound **2** (39:61 *cis-P,F*:*trans-P,F* mixture) reacts quantitatively with VF in CD_2Cl_2 solution to yield the insertion product (PO-OMe)-Pd(CH_2CHF_2)(lut) (**3**, Scheme 3). The ^1H and ^{19}F NMR spectra of **3** contain characteristic signals for the PdCH_2CHF_2 unit (^1H NMR δ 4.84 (tt, $^2J_{FH}$ = 57, $^3J_{HH}$ = 5, PdCH$_2$C*H*F$_2$), δ 1.06 (tdd (apparent tt), $^3J_{FH}$ = 22, $^3J_{PH}$ = 6, $^3J_{HH}$ = 5, PdC*H*$_2$CHF$_2$); ^{19}F NMR δ −98.3 (d, $^2J_{FH}$ = 57)) that are similar to those observed for the analogous complex **A**.[6] Complex **3** exists as the *cis-P,C* isomer, as established by a room temperature NOESY correlation between the PdC*H*$_2$CHF$_2$ hydrogens and the hydrogens *ortho* to P on the 2-OMe-Ph rings (H^6) and the small J_{PC} value (<5 Hz) for the PdCH$_2$CHF$_2$ carbon.

^1H NMR monitoring of the reaction of **2** (39:61 *cis-P,F*:*trans-P,F* mixture) and VF shows that *cis-P,F*-**2** reacts faster

DOI: 10.1021/acs.organomet.9b00545
Organometallics 2019, 38, 4250−4260

Scheme 3. Reaction of 2 and VF to Produce 3

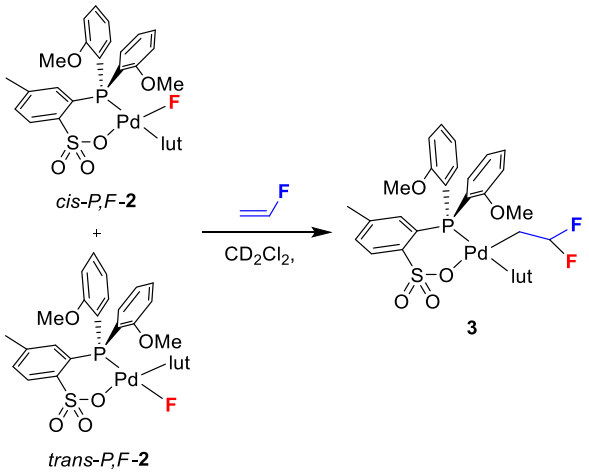

than *trans-P,F*-**2**. At room temperature after 20 h, *cis-P,F*-**2** was completely consumed and a 49:51 mixture of **3** and *trans-P,F*-**2** was present. After 44 h, a 61:39 mixture of **3** and *trans-P,F*-**2** was present. Heating the sample tube at 40 °C for an additional 22 h gave **3** in >95% yield.

Reaction of 2 with Vinyl Bromide. Complex **2** (1:1 *cis-P,F*:*trans-P,F* mixture) reacts with VBr in CD_2Cl_2 solution to give **1** and VF (Scheme 4). This reaction likely proceeds by

Scheme 4. Reaction of 2 with VBr

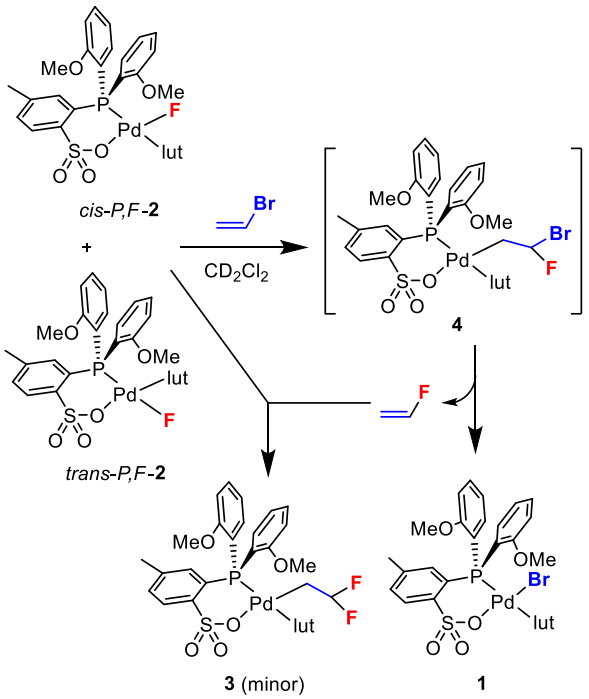

initial fluoropalladation to form (PO-OMe)Pd(CH_2CHBrF)(lut) (**4**) followed by *β*-Br elimination. Intermediate **4** is not observed, indicating that *β*-Br elimination is faster than the initial fluoropalladation step. After 13 h at 50 °C, the reaction mixture contained **1** (73% by ^{31}P NMR), **3** (11%), and *cis-P,F*-**2** (7%). The presence of **3**, which is formed by the reaction of **2** with the VF that is released by *β*-Br elimination, indicates that VF and VBr react with **2** at comparable rates. Assuming that *cis-P,F*-**2** reacts faster with VBr than does *trans-P,F*-**2**, as is the case for VF and VOAc (vide infra), the *cis-P,F*-**2** that is present at the end of the reaction likely forms by *β*-F elimination of **3** or **4**.

Reaction of 2 with Vinyl Acetate and Vinyl Benzoate. Compound **2** (70:30 *cis-P,F*:*trans-P,F* mixture) reacts with VOAc in CD_2Cl_2 solution at 50 °C in a sealed tube to yield the insertion product (PO-OMe)Pd{$CH_2CHF(OAc)$}(lut) (**5**, Scheme 5). Under these conditions, **5** reacts further to form

Scheme 5. Reaction of 2 and VOAc and VOBz (R = Me or Ph)

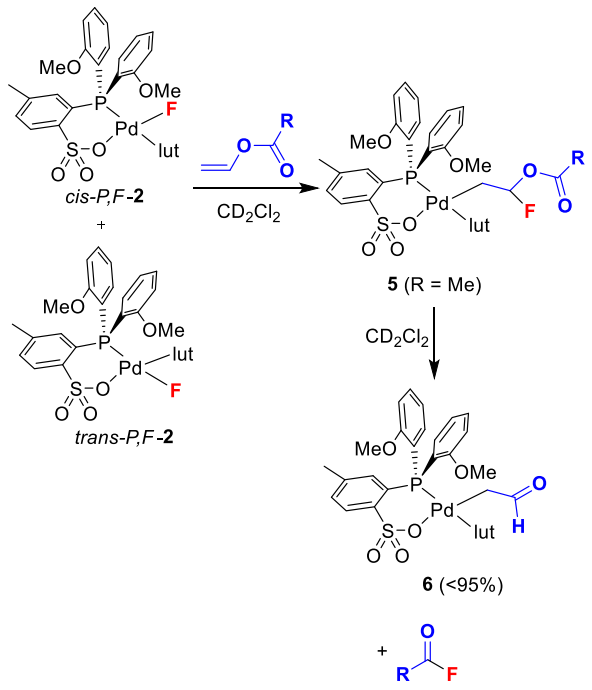

the C-bound enolate complex (PO-OMe)Pd{$CH_2C(=O)H$}(lut) (**6**, >95% by ^{31}P NMR) and acetyl fluoride (1 equiv vs **6**; ^{19}F NMR δ 50.5; ^{1}H NMR δ 2.2 (d, $^{3}J_{FH}$ = 7 Hz)) without observable intermediates.[14] NMR monitoring experiments show that *cis-P,F*-**2** reacts faster than *trans-P,F*-**2**. After 2.2 h at 50 °C, 100% of *cis-P,F*-**2** and 67% of *trans-P,F*-**2** had reacted resulting in an overall 78% conversion to **5**. After 10 h, **5** and the remaining *trans-P,F*-**2** had reacted resulting in >95% conversion to **6**.

The ^{1}H NMR spectra of **5** are similar to those of VF insertion product **3**. The signals for the PO-OMe and lut ligands of the two complexes are nearly identical, and the resonances for the $PdCH_2CHF(OAc)$ ligand of **5** (δ 5.36 (dt, $^{2}J_{FH}$ = 58, $^{3}J_{HH}$ = 5.5, 1H, $PdCH_2CHF(OAc)$) and 1.06 (m, 2H, $PdCH_2CHF(OAc)$) are similar to those for the $PdCH_2CHF_2$ ligand in **3**. The multiplicities and coupling constants are consistent with the presence of one fluorine atom in **5**. The ^{1}H NMR spectrum of **6** contains a signal at δ 8.54 (t, $^{3}J_{HH}$ = 5 Hz) for the aldehydic hydrogen and a signal at δ 1.84 (dd, $^{3}J_{PH}$ = 5, $^{3}J_{HH}$ = 5) for the $PdCH_2C(=O)H$ hydrogens.

The analogous reaction of **2** (42:58 *cis-P,F*:*trans-P,F* mixture) and vinyl benzoate (VOBz) in CD_2Cl_2 (60 °C, sealed tube) produced **6** in high yield along with PhC(=O)F (1 equiv vs **6**; ^{19}F NMR δ 17.4).

Crystals of **6**·1.5(CH_2Cl_2) were obtained by layering pentane over the CD_2Cl_2 solution at the end of the reaction of **2** with VOAc and cooling the mixture at −40 °C. The

DOI: 10.1021/acs.organomet.9b00545
Organometallics 2019, 38, 4250−4260

molecular structure and selected metrical data are shown in Figure 2. The C—C (1.468(9) Å) and C═O (1.216(8) Å)

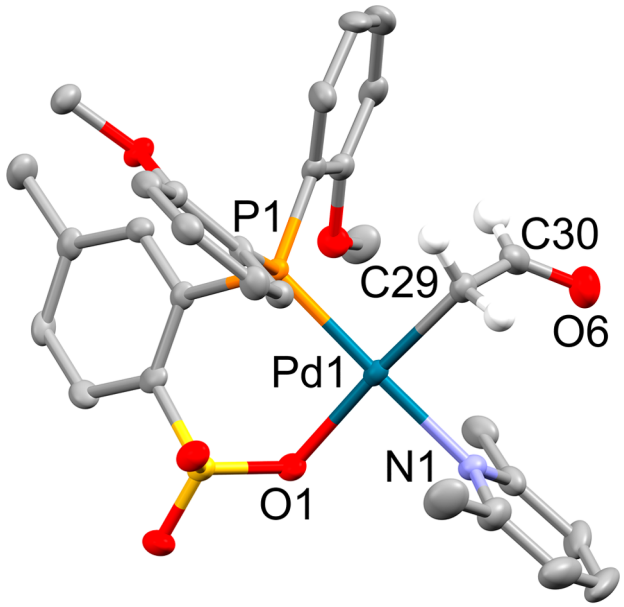

Figure 2. Molecular structure of **6**·1.5(CH_2Cl_2). Hydrogen atoms on the CH_2(C═O)H ligand were calculated using displacement parameters set to 1.2 times the isotropic equivalent of the displacement parameters of the bonded atoms. All other hydrogen atoms and the CH_2Cl_2 molecules are omitted for clarity. Bond lengths (Å) and angles (deg): Pd1−C29 2.065(6), Pd1−N1 2.121(5), Pd1−O1 2.114(4), Pd1−P1 2.2391(16), C29−C30 1.468(9), O6−C30 1.216(8), C29−Pd1−N1 90.1(2), N1−Pd1−O1 86.45(17), C29−Pd1−P1 88.96(18), O1−Pd1−P1 94.56(12).

bond distances in **6** are similar to those in aldehydes (1.51 and 1.19 Å),[15] and other C-bound enolate complexes, such as (Tp*)Ir(CO){CH_2C(═O)H}$_2$ (Tp* = HB($C_3N_2HMe_2$)$_3$; 1.429(8) and 1.206(7) Å),[16] and (tpy)Au{OAc^F}{CH_2C(═O)H} (tpy = 2-(*p*-tolyl)pyridine, OAc^F = OC(═O)CF_3; 1.468(3) and 1.212(3) Å).[17,18]

The conversion of **5** to **6** may proceed by direct elimination of acetyl fluoride from **5.** Several similar reactions have been reported previously. Nova and Tilset reported that (tpy)Au(OAc^F){$CH_2CH(OAc^F)_2$}, which was generated in situ by two different routes, reacts to form the C-bound enolate complex (tpy)Au(OAc^F){CH_2C(═O)H} and trifluoroacetic anhydride, and proposed a direct elimination mechanism for this process.[17] Similar acid-catalyzed eliminations have been used to interconvert 1,1-diacetates and the corresponding aldehydes and acetic anhydride.[19]

DFT Analysis of the Reaction of Model (PO)PdF(py) Complexes with VF and VBr. Two principal mechanisms are possible for the fluoropalladation of olefins by (PO-OMe)PdF(lut) (**2**): (i) substitution of lutidine by olefin followed by migratory insertion into the Pd−F bond, and (ii) substitution of fluoride by olefin to generate a (PO-OMe)Pd(olefin)(lut)$^+$ species and free (solvated) F^-, followed by exo attack of F^- on the olefin (Scheme 6).[20] These processes have been investigated by density functional theory (DFT) using the simple model complexes *cis-P,F*-(PH_2O)-PdF(py) (**C1**) and *trans-P,F*-(PH_2O)PdF(py) (**C2**), which contain the parent phosphine-arenesulfonate ligand *o*-$PH_2C_6H_4SO_3^-$ (PH_2O^-). This model ligand system was

Scheme 6. Possible Mechanisms for Fluoropalladation of CH_2═CHX by (PO-OMe)PdF(lut) (2)

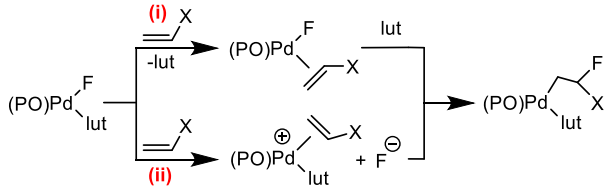

selected to minimize the influence of steric effects arising from the phosphine substituents.[21−23]

Figure 3 shows the computed potential energy surface for the migratory insertion of VF into the Pd−F bond of model complexes **C1** and **C2**. The highest barriers on this surface are those for isomerization of **C1** and **C2** and isomerization of **C3** to **C7** (not shown; see Supporting Information). Fluoropalladation proceeds by associative substitution of py by VF to generate *cis-P,F* and *trans-P,F*-(PH_2O)PdF(VF) (**C7**, **C3**) followed by insertion and trapping by py to afford *cis-P,F* and *trans-P,F*-(PH_2O)Pd(CH_2CHF_2)(py) (**C9**, **C5**). Consistent with the expected kinetic and thermodynamic *trans* effects arising from the presence of the strong phosphine and the weak sulfonate donors, the barrier for displacement of py by VF from **C1** is lower than that for **C2**, and the Pd−C distances in **C7** (where VF is *trans* to P; 2.302 and 2.396 Å) are longer than those in **C3** (where VF is *trans* to O; 2.196 and 2.170 Å). The conversions of **C1** and **C2** to **C7** and **C3** are endergonic by ca. 12−13 kcal/mol. Migratory insertion of **C7** to produce the *β*-F datively chelated, *trans-P,C* species **C8** has a modest barrier (19.0 kcal/mol) and is endergonic by 16 kcal/mol, while insertion of **C3** to produce *cis-P,C* species **C4** has a lower barrier (11.4 kcal/mol) and is nearly isoergonic. Similar results were observed for analogous insertions of (PO)PdR(CH_2═CH_2) complexes.[21b] **C9**, the initial product from fluoropalladation of **C1**, is computed to undergo facile isomerization to **C5** ($\Delta E^{\ddagger}$ = 24 kcal/mol). These results are consistent with the experimental observations that the isomerization of *cis-P,F-* and *trans-P,F-***2** is slow and *cis-P,C-***4** is the sole product in the reaction of **2** with VF. These results show that the migratory insertion mechanism is a reasonable pathway for the reaction of **2** with VF.

Computational analysis of the exo attack mechanism (mechanism ii in Scheme 6) is challenging because the Coulombic attraction dominates the intermolecular forces during the gas phase geometry optimization steps. However, polarizable continuum models (PCMs) have been used successfully to model the influence of solvent on reactions and to model the attack of anions on olefins and alkynes coordinated to transition metals.[17,24−27] Using this approach, the displacement of fluoride from **C1** and **C2** is predicted to be highly energetically unfavorable (ΔE > 46 kcal/mol), ruling out this mechanism as a viable process (Figure 4).

The computed potential energy profiles for the insertion of the model VBr adducts *cis-P,F-* and *trans-P,F*-(PH_2O)PdF-(VBr) (**C17**, **C13**) are shown in Figure 5. Consistent with the results for VF insertion, the insertion of the *cis-P,F* isomer **C17** to produce the *β*-F datively chelated, *trans-P,C* species **C18** has a barrier of 20.6 kcal/mol and is endergonic, while the corresponding reaction of the *trans-P,F* isomer **C13** to produce *cis-P,C* isomer **C14** has a low barrier (12.9 kcal/mol) and is nearly isoergonic. **C14** undergoes fast isomerization to the *β*-Br-chelated isomer **C15** followed by *β*-Br elimination to

DOI: 10.1021/acs.organomet.9b00545
Organometallics 2019, 38, 4250−4260

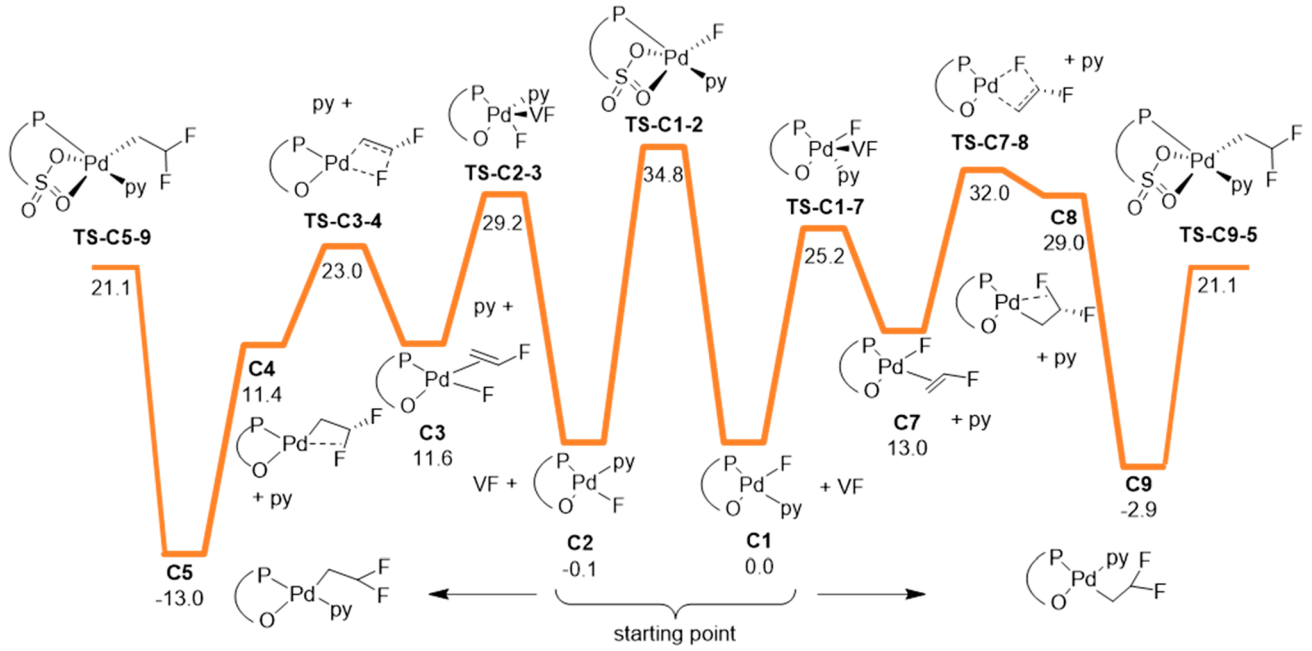

Figure 3. Computed potential energy surface for the reaction of model compounds *cis-P,F*-(PH_2O)PdF(py) (**C1**) and *trans-P,F*-(PH_2O)PdF(py) (**C2**) with VF. Potential energies are calculated in CH_2Cl_2 and reported in kcal/mol.

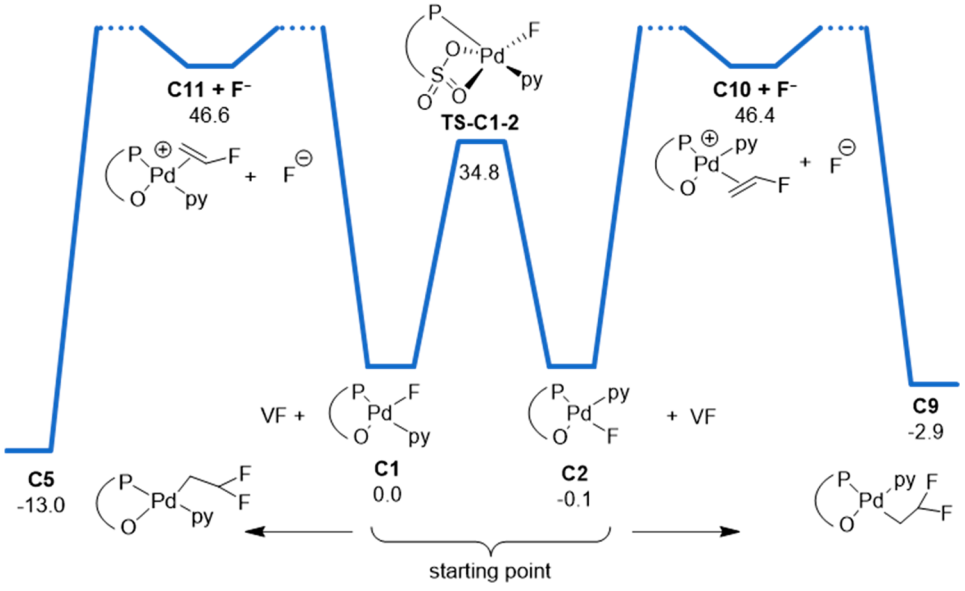

Figure 4. Potential energy surface for the reaction of *cis-P,F*-(PH_2O)PdF(py) (**C1**) and *trans-P,F*-(PH_2O)PdF(py) (**C2**) with VF via an exo attack mechanism. Potential energies are calculated in CH_2Cl_2 and reported in kcal/mol. Transition state energies are estimated at 5 kcal/mol greater than the energies of the intermediate species **C11** and **C10** and fluoride.

produce Pd−Br complex **C16**. Attempted location/optimization of the *β*-Br-chelated intermediate and *β*-Br elimination transition state for the *trans-P,C* isomer **C18** resulted in Pd bromide product **C12**, implying that the barrier to *β*-Br elimination is quite low. These results suggest that a migratory insertion/*β*-Br elimination mechanism is a reasonable pathway for the observed formation of **1** from the reactions of **2** with VBr. Also, these results are consistent with DFT calculations for $[L_2PdCH_2CH_2Br]^+$ ($L_2 = H_2PCH_2CH_2PH_2$), which predict that *β*-Br elimination is exothermic and proceeds with a small barrier of 1.9 kcal/mol.[28] In contrast, *β*-F elimination of $[L_2PdCH_2CH_2F]^+$ is endothermic due to the strong C−F bond and relatively weak Pd−F bond in the *β*-F elimination product and has a higher barrier of 14.0 kcal/mol.

CONCLUSION

The (phosphine-arenesulfonate)Pd(II) fluoride complex (PO-OMe)PdF(lut) (**2**) exists as a mixture of *cis-P,F* and *trans-P,F* isomers that interconvert slowly in solution and in the solid state. Compound **2** reacts with electron-deficient olefins to afford net 1,2-insertion products. The vinyl fluoride insertion product **3** is stable, while the vinyl bromide insertion product **4**, which was not observed, undergoes rapid *β*-Br elimination to afford (PO-OMe)PdBr(lut) (**1**) and vinyl fluoride. The vinyl acetate insertion product **5** undergoes elimination of

DOI: 10.1021/acs.organomet.9b00545
Organometallics 2019, 38, 4250−4260

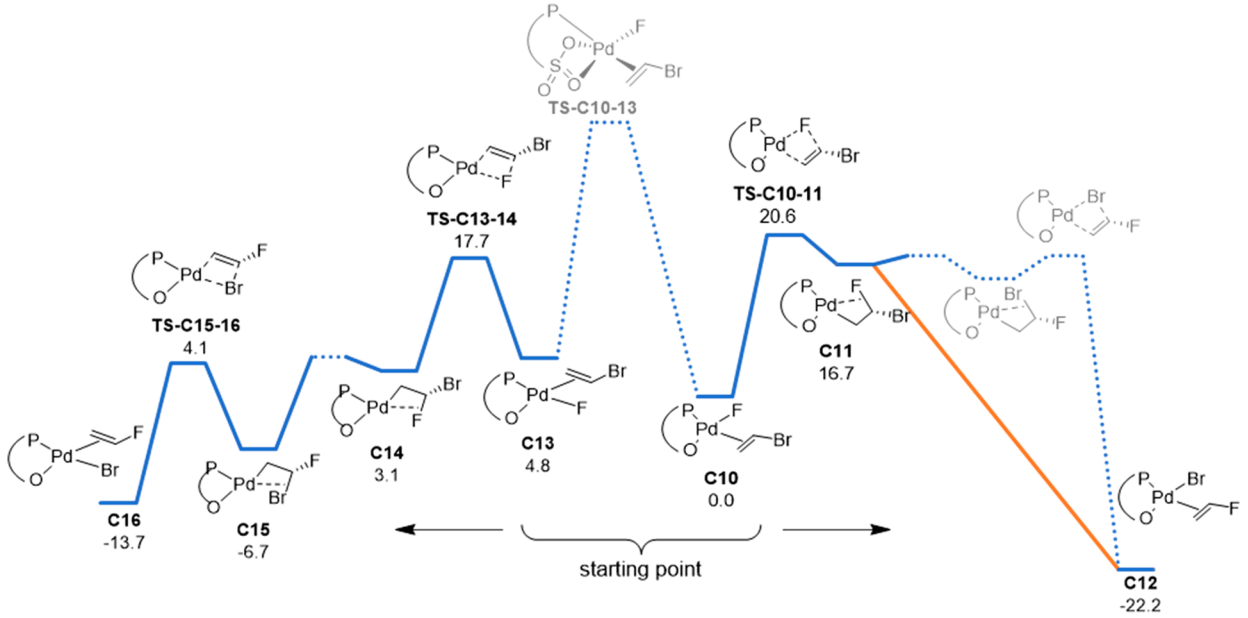

Figure 5. Potential energy surface for the insertion and β-Br elimination mechanism for the reaction of *cis-P,F* and *trans-P,F*-$(PH_2O)PdF(VBr)$ (**C17** and **C13**). Paths with dotted lines are estimates based on previous calculations. Attempted location/optimization of the β-Br-chelated intermediate and β-Br elimination transition state for the *trans-P,C* isomer **C18** resulted in Pd bromide product **C12**, implying that the barrier to β-Br elimination is quite low. Dotted lines show an estimate of the energetics of the reaction path that were not located.

acetyl fluoride to afford C-bound Pd-enolate complex **6**. DFT analysis of the reaction of the model complexes *cis-P,F-* and *trans-P,F*-$(PH_2O)PdF(py)$ (**C1** and **C2**, PH_2O^- = *o*-$PH_2C_6H_4SO_3^-$) with VF supports a mechanism involving substitution of lutidine by VF followed by migratory insertion into the Pd−F bond. DFT analysis of the reaction of the model complexes *cis-P,F-* and *trans-P,F*-$(PH_2O)PdF(VBr)$ (**C17**, **C13**) supports an insertion/β-Br elimination mechanism. Taken together with the previous observation of ethylene and VF insertion of $(PO^{Bp,OMe})Pd(CH_2CHF_2)(lut)$ (**B**),[6] these results suggest that olefin insertion is a general reactivity mode for (PO)Pd fluoride complexes. The high insertion reactivity of (PO)PdF species reflects the nucleophilic character of the Pd-*F* ligand.

EXPERIMENTAL SECTION

General Procedures. All experiments were performed using drybox or Schlenk techniques under a nitrogen atmosphere unless noted otherwise. Nitrogen was purified by passage through Q-5 oxygen scavenger and activated molecular sieves. CH_2Cl_2, Et_2O, and THF were dried by passage through activated alumina. Pentane was purified by passage through BASF R3−11 oxygen scavenger and activated alumina. CD_2Cl_2 and $CDCl_2CDCl_2$ were dried over and distilled from P_2O_5 or used as received from an ampule. ^{n}BuLi solution (1.6 or 2.5 M in hexanes), 2-bromoanisole, $(COD)PdBr_2$, 2,6-lutidine (99+%), CsF, vinyl bromide (VBr, 1 M, THF), vinyl acetate (VOAc), and $[NBu_4]Br$ were purchased from Sigma-Aldrich. $[NBu_4]Br$ was recrystallized from hot toluene and VOAc was distilled from $CaCl_2$ before being stored in a glovebox. Other materials were used without further purification. Vinyl fluoride was purchased from Synquest Laboratories and used as received. $HP^+(2\text{-OMe-Ph})_2(2\text{-}SO_3^-\text{-5-Me-Ph})$ was prepared by the literature procedure.[29]

The fluoride ligands in Pd−F complexes are highly basic and nucleophilic and a locus for H bonding.[13b] In solution, Pd−F complexes can generate free fluoride (^{19}F NMR δ −129)[30] and can be hydrolyzed by trace water to form HF, which can react with borosilicate glass to generate fluorosilicate species (^{19}F NMR δ −153).[31] To avoid these problems, polypropylene (PP) containers and funnels and Teflon filtration flasks and NMR tube liners were used for the synthesis, storage, analysis, and reactions of **2**.

NMR spectra were recorded on Bruker Avance II+ 500 or DRX400 spectrometers at ambient temperature unless otherwise indicated. ^{1}H and ^{13}C chemical shifts are reported relative to $SiMe_4$ and internally referenced to residual ^{1}H and ^{13}C solvent resonances. ^{31}P chemical shifts are externally referenced to 85% H_3PO_4(δ 0.0). ^{19}F chemical shifts are externally referenced to $BF_3(OEt_2)$ (δ −153 for ^{19}F).

Electrospray mass spectra (ESI-MS) were recorded using an Agilent 6224 TOF−MS (high resolution) instrument. The observed isotope patterns closely matched calculated isotope patterns. The listed *m/z* value corresponds to the most intense peak in the isotope pattern.

Synthesis of Complexes. *{P(2-OMe-Ph)$_2$(2-SO$_3$-5-Me-Ph)}PdBr-(2,6-lutidine) (**1**, (PO-OMe)PdBr(lut)).* A solution of $HP^+(2\text{-OMe-Ph})_2(2\text{-}SO_3^-\text{-5-Me-Ph})$(2.41 g, 5.80 mmol) in CH_2Cl_2 (60 mL) was added dropwise to a solution of $(COD)PdBr_2$ (2.16 g, 5.80 mmol) in CH_2Cl_2 (30 mL). The solution was stirred for 1.5 h at room temperature. Lutidine (1.34 mL, 11.6 mmol) was added dropwise and the mixture was stirred for 30 min at room temperature. Pentane (600 mL) was added and an orange precipitate formed. The orange powder was collected by filtration, washed with pentane, and recrystallized from CH_2Cl_2/Et_2O (100 mL/300 mL) at −40 °C to afford orange crystals, which were identified as $(PO\text{-}OMe)PdBr(lut)\cdot CH_2Cl_2$ (**1**·CH_2Cl_2) by X-ray crystallography. The crystals were collected by filtration and dried under a vacuum to afford **1**. Yield 3.62 g (86.2% based on $(COD)PdBr_2$). X-ray quality orange crystals identified as **1**·CH_2Cl_2 were also grown from a concentrated CH_2Cl_2 solution of **1** at room temperature. The atom numbering scheme used in the NMR assignments of **1** is shown in Figure 6. ^{1}H NMR (CD_2Cl_2) δ 8.03 (br s, 2H, H^6), 7.83 (dd, $^3J_{HH}$ = 8, $^4J_{PH}$ = 5, 1H, H^9), 7.62 (t, $^3J_{HH}$ = 8, 1H, H^{15}), 7.60 (t, $^3J_{HH}$ = 8, 2H, H^4), 7.32 (d, $^3J_{HH}$ = 8, 1H, H^{10}), 7.16 (d, $^3J_{HH}$ = 8, 2H, H^{14}), 7.12 (d, $^3J_{PH}$ = 14, 1H, H^{12}), 7.11 (t, $^3J_{HH}$ = 8, 2H, H^5), 6.79 (dd, $^3J_{HH}$ = 8, $^4J_{PH}$ = 5, 2H, H^3), 3.67 (s, 6H, H^{18}), 3.31 (s, 6H, H^{16}), 2.29 (s, 3H, H^{17}). ^{13}C{^{1}H} NMR (CD_2Cl_2) δ 160.6 (C^2), 159.4 (C^{13}), 143.9 (d, $^2J_{PC}$ = 13, C^8), 139.6 (C^{11}), 139.3 (C^{15}),138.8 (br, C^6), 135.4 (C^{12}), 134.4 (C^4), 131.7 (C^{10}), 127.2 (d, $^2J_{PC}$ = 9, C^9), 126.6 (d, $^1J_{PC}$ = 53, C^7), 123.4 (C^{14}), 120.7 (d, $^3J_{PC}$ = 12, C^5), 115.0 (d, $^1J_{PC}$ = 64, C^1), 111.8 (C^3), 55.5 (C^{18}), 26.0 (C^{16}), 21.4 (C^{17}). ^{31}P{^{1}H} NMR (CD_2Cl_2) δ 4.6 (s). HRMS (ESI mode; *m/*

DOI: 10.1021/acs.organomet.9b00545
Organometallics 2019, 38, 4250−4260

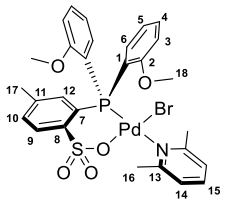

Figure 6. Atom numbering scheme for **1**.

z) calcd for $[C_{28}H_{30}BrNO_5PPdS]^+$ ($[M + H]^+$) 709.9792, found 709.9788.

*{P(2-OMe-Ph)$_2$(2-SO$_3$-5-Me-Ph)}PdF(2,6-lutidine) (**2**, (PO-OMe)-PdF(lut))*. In a dark glovebox, AgF (0.208 g, 1.64 mmol) was added to an orange solution of **1** (0.397 g, 0.548 mmol) in CH_2Cl_2 (15 mL) in a foil-wrapped PP vial. An excess of AgF was used because AgF is only sparingly soluble in CH_2Cl_2. The mixture was stirred for 20 h at room temperature. The dark brown slurry was gravity filtered through filter paper into a Teflon filtration flask to remove the brown-black AgX powder. The volatiles were removed under a vacuum and the resulting tan solid was transferred to a PP vial and stored at −40 °C. Yield: 0.338 g, 95.3%. The crude material was enriched in *cis-P,F*-**2** (82:18 *cis*:*trans-P,F*), but a 44:56 *cis*:*trans-P,F* mixture formed over 1 month while the solid was stored at −40 °C. The atom numbering scheme used in the NMR assignments of **2** is shown in Figure 7. NMR data

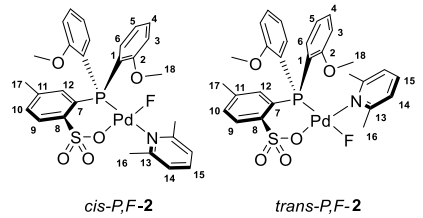

Figure 7. Atom numbering scheme for *cis-P,F* and *trans-P,F*-**2**.

for *cis-P,F*-**2**: ^{1}H NMR (CD_2Cl_2) δ 7.81 (dd, $^3J_{HH}$ = 8, $^4J_{PH}$ = 5, 1H, H^9), 7.75 (br s, 2H, H^6), 7.65 (t, $^3J_{HH}$ = 8, 2H, H^4), 7.63 (t, $^3J_{HH}$ = 8, 1H, H^{15}), 7.37 (d, $^3J_{HH}$ = 8, 1H, H^{10}), 7.16 (d, $^3J_{HH}$ = 8, 2H, H^{14}), 7.11 (d, $^3J_{PH}$ = 6.5, 1H, H^{12}), 7.06 (t, $^3J_{HH}$ = 8, 2H, H^5), 7.03 (d, $^3J_{HH}$ = 8, 2H, H^3), 3.71 (s, 6H, H^{18}), 3.45 (s, 6H, H^{16}), 2.32 (s, 3H, H^{17}). ^{13}C{^{1}H} NMR (CD_2Cl_2) δ 161.0 (C^2), 159.6 (C^{13}), 143.5 (br s, C^8), 140.1 (C^{11}), 139.4 (C^{15}), 137.5 (C^6), 136.3 (C^{12}), 134.6 (C^4), 132.0 (C^{10}), 127.3 (C^9), 126.7 (d, $^1J_{PC}$ = 52, C^7), 123.2 (C^{14}), 121.4 (d, $^3J_{PC}$ = 11, C^5), 114.7 (d, $^1J_{PC}$ = 56, C^1), 111.8 (C^3), 55.8 (C^{18}), 24.0 (C^{16}), 21.4 (C^{17}). ^{31}P{^{1}H} NMR (CD_2Cl_2) δ −4.7 (d, $^2J_{PF}$ = 16). ^{19}F{^{1}H} NMR (CD_2Cl_2, − 15 °C) δ −436 (d, $^2J_{PF}$ = 16). NMR data for *trans-P,F*-**2**: ^{1}H NMR (CD_2Cl_2) δ 7.96 (dd, $^3J_{HH}$ = 8, J_{PH} = 5, 1H, H^9), 7.75 (br s, 2H, H^6), 7.52 (t, $^3J_{HH}$ = 8, 2H, H^4), 7.46 (d, $^3J_{HH}$ = 8, 1H, H^{10}), 7.36 (t, $^3J_{HH}$ = 7, 1H, H^{15}), 7.11 (d, $^3J_{PH}$ = 6.5, 1H, H^{12}), 7.10 (t, $^3J_{HH}$ = 8, 2H, H^5), 6.81 (d, $^3J_{HH}$ = 7, 2H, H^{14}), 6.74 (d, $^3J_{HH}$ = 8, 2H, H^3), 3.43 (s, 6H, H^{18}), 3.06 (s, 6H, H^{16}), 2.24 (s, 3H, H^{17}). ^{13}C{^{1}H} NMR (CD_2Cl_2) δ 161.2 (C^{13}), 160.4 (C^2), 145.6 (d, $^2J_{PC}$ = 14, C^8), 140.4 (C^{11}), 139.5 (C^{15}), 137.5 (C^6), 135.4 (C^4), 133.9 (C^{12}), 133.5 (C^{10}), 128.0 (C^9), 128.0 (d, $^1J_{PC}$ = 52, C^7), 122.9 (C^{14}), 121.8 (d, $^3J_{PC}$ = 7, C^5), 114.7 (d, $^1J_{PC}$ = 56, C^1), 111.8 (C^3), 55.4 (C^{18}), 27.1 (C^{16}), 21.3 (C^{17}). ^{31}P{^{1}H} NMR (CD_2Cl_2) δ 3.0 (d, $^2J_{PF}$ = 210). ^{19}F{^{1}H} NMR (CD_2Cl_2) δ −267 (d, $^2J_{PF}$ = 210). HRMS (ESI mode; *m*/*z*) calcd for $[C_{28}H_{29}NO_5PPdS]^+$ ($[M - F]^+$) 628.0544, found 628.0560.

*{P(2-OMe-Ph)$_2$(2-SO$_3$-5-Me-Ph)}Pd(CH$_2$CF$_2$H)(2,6-lutidine) (**3**, (PO-OMe)PdCH$_2$CF$_2$H(lut))*. A Teflon NMR tube liner was charged with **2** (10 mg, 0.015 mmol, 39:61 *cis-P,F*:*trans-P,F*) and CD_2Cl_2 (0.3 mL). The liner was sealed in a J-Young tube. Vinyl fluoride (20 mL gas bulb, 129 mm Hg of VF, 1.5 equiv) was condensed into the tube. The tube was warmed to room temperature and monitored by NMR. After 20 h, *cis-P,F*-**2** was completely consumed and a 54:46 mixture of *trans-P,F*-**2** and **3** was present. The tube was heated at 40 °C for 22.5 h, during which time the remaining *trans-P,F*-**2** was converted to **3**. The atom numbering scheme for **3** is shown in Figure 8. Figure S9 shows NMR monitoring of this reaction. The NMR spectra used to

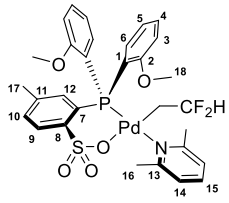

Figure 8. Atom numbering scheme for **3**.

make assignments for **3** are those from the end of this reaction mixture (>90% pure, Figure S11). Iterative line fitting using gNMR 5.0 was done on the resonance at 1.06 ppm to determine coupling constants. ^{1}H NMR (CD_2Cl_2) δ 7.87 (dd, $^3J_{HH}$ = 8, $^4J_{PH}$ = 5, 1H, H^9), 7.74 (br s, 2H, H^6), 7.66 (t, $^3J_{HH}$ = 8, 1H, H^{15}), 7.60 (t, $^3J_{HH}$ = 8, 2H, H^4), 7.30 (d, $^3J_{HH}$ = 8, 1H, H^{10}), 7.19 (d, $^3J_{HH}$ = 8, 2H, H^{14}), 7.17 (d, $^3J_{PH}$ = 13, 1H, H^{12}), 7.11 (t, $^3J_{HH}$ = 8, 2H, H^5), 7.01 (dd, $^3J_{HH}$ = 8, $^4J_{PH}$ = 5, 2H, H^3), 4.84 (tt, $^2J_{FH}$ = 57, $^3J_{HH}$ = 5, 1H, PdCH$_2$C*H*F$_2$), 3.66 (s, 6H, H^{18}), 3.25 (s, 6H, H^{16}), 2.28 (s, 3H, H^{17}), 1.06 (ttd (apparent tt), $^3J_{FH}$ = 22, $^3J_{PH}$ = 6, $^3J_{HH}$ = 5, 2H, PdC*H*$_2$CHF$_2$). ^{13}C{^{1}H} NMR (CD_2Cl_2) δ 160.8 (C^2), 159.5 (C^{13}), 145.2 (d, $^2J_{PC}$ = 15, C^8), 139.2 (C^{11}), 139.1 (C^{15}),138.0 (C^6), 135.4 (C^{12}), 134.2 (C^4), 131.3 (C^{10}), 127.7 (C^9), 126.7 (d, $^1J_{PC}$ = 52, C^7), 123.2 (C^{14}), 121.1 (d, $^3J_{PC}$ = 11, C^5), 120.1 (t, $^1J_{CF}$ = 237, PdCH$_2$CHF$_2$), 114.7 (d, $^1J_{PC}$ = 56, C^1), 111.6 (C^3), 55.4 (C^{18}), 26.0 (C^{16}), 21.4 (C^{17}), 12.7 (t, $^2J_{CF}$ = 14, PdCH$_2$CHF$_2$). ^{31}P{^{1}H} NMR (CD_2Cl_2) δ 15.8 (s). ^{19}F NMR (CD_2Cl_2) δ −98.3 (d, $^2J_{FH}$ = 57). HRMS (ESI mode; *m*/*z*) calcd for $[C_{53}H_{56}F_4NO_{10}P_2Pd_2S_2]^+$ ($[2M - \text{lutidine} + H]^+$) 1282.0845, found 1282.0818.

*{P(2-OMe-Ph)$_2$(2-SO$_3$-5-Me-Ph)}Pd{CH$_2$CF(OAc)H}(2,6-lutidine) (**5**, (PO-OMe)Pd{CH$_2$CF(OAc)H}(lut))*. A Teflon NMR tube liner was charged with **2** (21 mg, 0.033 mmol, 70:30 *cis-P,F*:*trans-P,F*) and CD_2Cl_2(0.25 mL). VOAc (46 μL, 0.49 mmol) was added via microsyringe and the Teflon liner was sealed in an NMR tube. The tube was heated at 50 °C for 2.3 h, during which time 78% **2** was converted to **5** (by ^{31}P NMR). NMR assignments for **5** were made by 1- and 2-D NMR analyses of this mixture. The numbering scheme for **5** is shown in Figure 9. ^{1}H NMR (CD_2Cl_2) δ 7.86 (dd, $^3J_{HH}$ = 8, $^4J_{PH}$

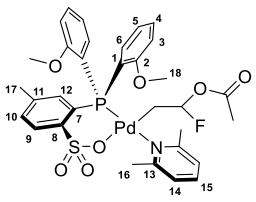

Figure 9. Atom numbering scheme for **5**.

= 5, 1H, H^9), 7.73 (br s, 2H, H^6), 7.65 (t, $^3J_{HH}$ = 8, 1H, H^{15}), 7.57 (t, $^3J_{HH}$ = 8, 2H, H^4), 7.30 (d, $^3J_{HH}$ = 8, 1H, H^{10}), 7.17 (d, $^3J_{HH}$= 8, 2H, H^{14}), 7.16 (d, $^3J_{PH}$ = 12, 1H, H^{12}), 7.09 (t, $^3J_{HH}$ = 8, 2H, H^5), 7.00 (dd, $^3J_{HH}$ = 8, $^4J_{PH}$ = 5, 2H, H^3), 5.36 (dt, $^2J_{FH}$ = 58, $^3J_{HH}$ = 5, 1H, PdCH$_2$C*H*F(OAc)), 3.66 (s, 3H, H^{18}), 3.65 (s, 3H, H^{18}), 3.17 (s, 3H, H^{16}), 3.16 (s, 3H, H^{16}), 2.26 (s, 3H, H^{17}), 2.26 (s, 3H, PdCH$_2$CHF(OC(O)C*H*$_3$), 1.06 (m, 2H, PdC*H*$_2$CHF(OAc)). ^{13}C{^{1}H} NMR (CD_2Cl_2) δ 168.8 (PdCH$_2$CHF(OC(O)CH$_3$)), 160.9 (C^2), 159.4 (C^{13}), 145.8 (C^8), 139.0 (C^{11}), 138.9 (C^{15}),138.2 (C^6), 135.4 (C^{12}), 134.1 (C^4), 131.3 (C^{10}), 127.7 (C^9), 126.8 (d, $^1J_{PC}$ = 51, C^7), 123.2 (C^{14}), 121.0 (d, $^3J_{PC}$ = 10, C^5), 114.8 (d, $^1J_{PC}$ = 54, C^1), 111.7 (C^3), 105.6 (d, $^1J_{FC}$ = 220, PdCH$_2$CHF(OAc)), 55.4 (C^{18}), 30.1 (PdCH$_2$CHF(OC(O)CH$_3$)), 26.1 (C^{16}), 21.3 (C^{17}), 12.4 (d, $^2J_{FC}$ = 17, PdCH$_2$CHF(OAc)). ^{31}P{^{1}H} NMR (CD_2Cl_2) δ 16.7 (s). ^{19}F{^{1}H} NMR (CD_2Cl_2) δ −108 (s).

*{P(2-OMe-Ph)$_2$(2-SO$_3$-5-Me-Ph)}Pd{CH$_2$C(=O)H}(2,6-lutidine) (**6**, (PO-OMe)Pd(CH$_2$C(=O)H)(lut))*. A Teflon NMR tube liner was

DOI: 10.1021/acs.organomet.9b00545
Organometallics 2019, 38, 4250−4260

charged with *cis-P,F:trans-P,F*-**2** (21 mg, 0.033 mmol, 66:34 *cis-P,F:trans-P,F*) and CD_2Cl_2 (0.25 mL). VOAc (46 μL, 0.49 mmol) was added via microsyringe and the Teflon liner was sealed in an NMR tube. The tube was heated at 60 °C for 12 h. NMR analysis revealed that **6** had formed in >95% yield (by ^{31}P NMR) along with acetyl fluoride (1 equiv vs **6**; ^{19}F NMR δ 50.5; ^{1}H NMR δ 2.2 (d, $^{3}J_{FH}$ = 7 Hz)). VF (<5% vs **6** by ^{19}F NMR and trace in ^{1}H NMR), and **6** (<5% by ^{31}P NMR) were also observed. X-ray quality crystals of **6**·1.5(CH_2Cl_2) were isolated (72% yield) by layering pentane onto this reaction mixture and cooling the tube to −40 °C. The numbering scheme for **6** is shown in Figure 10. ^{1}H NMR (CD_2Cl_2) δ 8.54 (t, $^{3}J_{HH}$ = 5, 1H, $PdCH_2C(=O)H$), 7.86 (dd, $^{3}J_{HH}$ = 8, $^{4}J_{PH}$ = 5, 1H, H^9), 7.71 (br s, 2H, H^6), 7.66 (t, $^{3}J_{HH}$ = 8, 1H, H^{15}), 7.57 (t, $^{3}J_{HH}$ = 8, 2H, H^4), 7.29 (d, $^{3}J_{HH}$ = 8, 1H, H^{10}), 7.18 (d, $^{3}J_{HH}$ = 8, 2H, H^{14}), 7.12 (d, $^{3}J_{PH}$ = 9, 1H, H^{12}), 7.10 (t, $^{3}J_{HH}$ = 8, 2H, H^5), 7.01 (dd, $^{3}J_{HH}$ = 8, $^{4}J_{PH}$ = 5, 2H, H^3), 3.69 (s, 6H, H^{18}), 3.14 (s, 6H, H^{16}), 2.28 (s, 3H, H^{17}), 1.84 (t, $^{3}J_{HH}$ = 5, $^{3}J_{PH}$ = 5, 2H, $PdCH_2C(=O)H$). $^{13}C\{^{1}H\}$ NMR (CD_2Cl_2) δ 208.8 ($PdCH_2C(=O)H$), 160.9 (C^2), 159.4 (C^{13}), 145.8 (C^8), 139.1 (C^{11}), 137.8 (C^{15}, C^6), 135.1 (C^{12}), 134.2 (C^4), 131.5 (C^{10}), 128.2 (C^9), 127.8 (d, $^{1}J_{PC}$ = 50, C^7), 123.4 (C^{14}), 121.1 (d, J_{PC} = 10, C^5), 114.8 (d, $^{1}J_{PC}$ = 52, C^1), 111.7 (C^3), 55.5 (C^{18}), 25.8 (C^{16}), 25.1 (C^{17}), 21.4 ($PdCH_2C(=O)H$). $^{31}P\{^{1}H\}$ NMR (CD_2Cl_2) δ 13.1 (s). HRMS (ESI mode; *m/z*) calcd for $[C_{30}H_{33}NO_6PPdS]^+$ ($[M + H]^+$) 672.0807, found 672.0814.

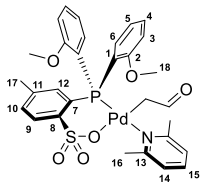

Figure 10. Atom numbering scheme for **6**.

■ ASSOCIATED CONTENT

Supporting Information

The Supporting Information is available free of charge on the ACS Publications website at DOI: 10.1021/acs.organomet.9b00545.

Additional experimental procedures, NMR data for compounds, computational details (PDF)

All computed molecule Cartesian coordinates in a format for convenient visualization (XYZ)

Accession Codes

CCDC 1944302 and 1944306 contain the supplementary crystallographic data for this paper. These data can be obtained free of charge via www.ccdc.cam.ac.uk/data_request/cif, or by emailing data_request@ccdc.cam.ac.uk, or by contacting The Cambridge Crystallographic Data Centre, 12 Union Road, Cambridge CB2 1EZ, UK; fax: +44 1223 336033.

■ AUTHOR INFORMATION

Corresponding Author

*E-mail: rfjordan@uchicago.edu.

ORCID

Rebecca E. Black: 0000-0002-3131-8228

Stefan M. Kilyanek: 0000-0002-6179-2510

Erik D. Reinhart: 0000-0003-2878-9376

Richard F. Jordan: 0000-0002-3158-4745

Author Contributions

Rebecca Black conducted the experimental work, Stefan Kilyanek carried out the DFT computations, Erik Reinhart performed HRMS experiments, and Richard Jordan directed the project.

Notes

The authors declare no competing financial interest.

■ ACKNOWLEDGMENTS

The authors thank Dr. Antoni Jurkiewicz assistance with NMR spectroscopy, Dr. Chang-Jin Qin for assistance with mass spectrometry, and Dr. Alexander Filatov for assistance with X-ray crystallography. This work was supported by National Science Foundation grants CHE-1709159 (RFJ) and CHE-16545 (SMK). This research was also supported by the Arkansas High Performance Computing Center, which is funded through National Science Foundation grants OAC-1440653, OIA-1457888. Additional funding was provided by the Arkansas Economic Development Commission and the University of Arkansas.

■ REFERENCES

(1) (a) Ahrens, T.; Kohlmann, J.; Ahrens, M.; Braun, T. Functionalization of Fluorinated Molecules by Transition-metal-mediated C-F Bond Activation to Access Fluorinated Building Blocks. *Chem. Rev.* **2015**, *115*, 931−972. (b) Liu, G. Transition Metal-catalyzed Fluorination of Multi Carbon-carbon Bonds: New Strategies for Fluorinated Heterocycles. *Org. Biomol. Chem.* **2012**, *10*, 6243−6248. (c) Ohashi, M.; Ogoshi, S. Catalytic Transformations of Fluorinated Olefins. In *Organometallic Fluorine Chemistry*; Braun, T., Hughes, R. P., Eds.; Topics in Organometallic Chemistry; Springer International Publishing: Cham, 2015; Vol. *52*, pp 197−215. (d) Orsi, D. L.; Altman, R. A. Exploiting the Unusual Effects of Fluorine in Methodology. *Chem. Commun.* **2017**, *53*, 7168−7181. (e) Landelle, G.; Bergeron, M.; Turcotte-Savard, M.-O.; Paquin, J.-F. Synthetic Approaches to Monofluoroalkenes. *Chem. Soc. Rev.* **2011**, *40*, 2867−2908. (f) Grushin, V. V. The Organometallic Fluorine Chemistry of Palladium and Rhodium: Studies Toward Aromatic Fluorination. *Acc. Chem. Res.* **2010**, *43*, 160−171. (g) Ohashi, M.; Saijo, H.; Shibata, M.; Ogoshi, S. Palladium-Catalyzed Base-Free Suzuki-Miyaura Coupling Reactions of Fluorinated Alkenes and Arenes via a Palladium Fluoride Key Intermediate. *Eur. J. Org. Chem.* **2013**, *2013*, 443−447.

(2) (a) Miller, W. T.; Fried, J. H.; Goldwhite, H. Substitution and Addition Reactions of the Fluoroölefins. IV. Reactions of Fluoride Ion with Fluoroölefins. *J. Am. Chem. Soc.* **1960**, *82*, 3091−3099. (b) Bayliff, A. E.; Chambers, R. D. Reactions Involving Fluoride Ion. Part 34. Stable Perfluorinated Carbanions. *J. Chem. Soc., Perkin Trans. 1* **1988**, *1*, 201. (c) Nguyen, B. V.; Burton, D. J. A New Route for the Preparation of Substituted 2,2-Difluorostyrenes and a Convenient Route to Substituted (2,2,2-Trifluoroethyl)benzenes. *J. Org. Chem.* **1997**, *62*, 7758−7764. (d) Chambers, R. D.; Nakamura, T. Reactions Involving Fluoride Ion. Part 47. Reactions of Perfluorobicycloalkenes. *J. Chem. Soc., Perkin Trans.* **2001**, *1*, 398−406. (e) Miller, W. T.; Freedman, M. B.; Fried, J. H.; Koch, H. F. Electrophilic Reactions of Argentous and Mercuric Fluorides with Fluoroölefins in Hydrogen Fluoride. *J. Am. Chem. Soc.* **1961**, *83*, 4105−4106. (f) Miller, W. T.; Burnard, R. J. Perfluoroalkylsilver Compounds. *J. Am. Chem. Soc.* **1968**, *90*, 7367−7368. (g) Miller, W. T.; Snider, R. H.; Hummel, R. J. Perfluoro-1-methylpropenylsilver. *J. Am. Chem. Soc.* **1969**, *91*, 6532−6534. (h) Banks, R. E.; Haszeldine, R. N.; Taylor, D. R.; Webb, G. Perfluoroprop-2-enylsilver. *Tetrahedron Lett.* **1970**, *11*, 5215−5216. (i) Dyatkin, B. L.; Martynov, B. I.; Martynova, L. G.; Kizim, N. G.; Sterlin, S. R.; Stumbrevichute, Z. A.; Fedorov, L. A. On the Interaction of Perfluoroalkyl Carbanions with Silver Salts. *J. Organomet. Chem.* **1973**, *57*, 423−433. (j) Krespan, C. G. Addition of Mercuric Fluoride to Fluoroethylenes. *J. Org. Chem.* **1960**, *25*, 105−107. (k) Aldrich, P. E.; Howard, E. G.; Linn, W. J.; Middleton, W. J.; Sharkey, W. H. Secondary and Tertiary Perfluoroörganomercury Compounds. *J. Org. Chem.* **1963**, *28*, 184−188. (l) Dyatkin, B. L.; Sterlin, S. R.; Martynov,

DOI: 10.1021/acs.organomet.9b00545
Organometallics 2019, 38, 4250−4260

B. I.; Mysov, E. I.; Knunyants, I. L. Reaction of Perfluoroalkyl Carbanions with Mercury Salts. *Tetrahedron* **1971**, *27*, 2843−2849. (m) Probst, A.; Raab, K.; Ulm, K.; von Werner, K. Synthesis and Chemistry of Perfluoro-2-iodo-2-methyl-alkanes. *J. Fluorine Chem.* **1987**, *37*, 223−245.

(3) (a) Loska, R.; Makosza, M. Synthesis of Perfluoroalkyl-substituted Azines via Nucleophilic Substitution of Hydrogen with Perfluoroisopropyl Carbanions. *J. Org. Chem.* **2007**, *72*, 1354−1365. (b) Riss, P. J.; Aigbirhio, F. I. A Simple, Rapid Procedure for Nucleophilic Radiosynthesis of Aliphatic [^{18}F]trifluoromethyl Groups. *Chem. Commun.* **2011**, *47*, 11873−11875. (c) Riss, P. J.; Ferrari, V.; Brichard, L.; Burke, P.; Smith, R.; Aigbirhio, F. I. Direct, Nucleophilic Radiosynthesis of [^{18}F]trifluoroalkyl Tosylates: Improved Labelling Procedures. *Org. Biomol. Chem.* **2012**, *10*, 6980−6986. (d) Gao, B.; Zhao, Y.; Ni, C.; Hu, J. AgF-mediated Fluorinative Homocoupling of Gem-difluoroalkenes. *Org. Lett.* **2014**, *16*, 102−105. (e) Hafner, A.; Feuerstein, T. J.; Bräse, S. Silver-mediated Methoxycarbonyltetrafluoroethylation of Arenes. *Org. Lett.* **2013**, *15*, 3468−3471. (f) Hafner, A.; Jung, N.; Bräse, S. Silver-Mediated Perfluoroalkylation Reactions. *Synthesis* **2014**, *46*, 1440−1447. (g) Gao, B.; Zhao, Y.; Hu, J. AgF-mediated Fluorinative Cross-coupling of Two Olefins: Facile Access to α-CF_3 Alkenes and β-CF_3 Ketones. *Angew. Chem., Int. Ed.* **2014**, *54*, 638−642. (h) Wang, X.; Li, Y.; Guo, Y.; Zhu, Z.; Wu, Y.; Cao, W. Direct Isoperfluoropropylation of Arenediazonium Salts with Hexafluoropropylene. *Org. Chem. Front.* **2016**, *3*, 304−308. (i) Li, Y.; Wang, X.; Guo, Y.; Zhu, Z.; Wu, Y.; Gong, Y. Direct Heptafluoroisopropylation of Arylboronic Acids via Hexafluoropropene (HFP). *Chem. Commun.* **2016**, *52*, 796−799.

(4) Akana, J. A.; Bhattacharyya, K. X.; Müller, P.; Sadighi, J. P. Reversible C-F Bond Formation and the Au-catalyzed Hydrofluorination of Alkynes. *J. Am. Chem. Soc.* **2007**, *129*, 7736−7737.

(5) (a) Qiu, S.; Xu, T.; Zhou, J.; Guo, Y.; Liu, G. Palladium-catalyzed Intermolecular Aminofluorination of Styrenes. *J. Am. Chem. Soc.* **2010**, *132*, 2856−2857. (b) Peng, H.; Yuan, Z.; Wang, H.; Guo, Y.; Liu, G. Palladium-catalyzed Intermolecular Fluoroesterification of Styrenes: Exploration and Mechanistic Insight. *Chem. Sci.* **2013**, *4*, 3172. (c) Peng, H.; Liu, G. Palladium-catalyzed Tandem Fluorination and Cyclization of Enynes. *Org. Lett.* **2011**, *13*, 772−775. (d) Yin, G.; Mu, X.; Liu, G. Palladium(II)-Catalyzed Oxidative Difunctionalization of Alkenes: Bond Forming at a High-Valent Palladium Center. *Acc. Chem. Res.* **2016**, *49*, 2413−2423. (e) Xu, T.; Qiu, S.; Liu, G. Palladium−Catalyzed Intramolecular Aminofluorination of Styrenes. *Chin. J. Chem.* **2011**, *29*, 2785−2790. (f) Kong, W.; Merino, E.; Nevado, C. Divergent Reaction Mechanisms in the Aminofluorination of Alkenes. *Chimia* **2014**, *68*, 430−435. (g) Chen, P.; Liu, G. Advancements in Aminofluorination of Alkenes and Alkynes: Convenient Access to β-Fluoroamines. *Eur. J. Org. Chem.* **2015**, *2015*, 4295−4309.

(6) Wada, S.; Jordan, R. F. Olefin Insertion into a Pd-F Bond: Catalyst Reactivation Following β-F Elimination in Ethylene/Vinyl Fluoride Copolymerization. *Angew. Chem., Int. Ed.* **2017**, *56*, 1820−1824.

(7) (a) Weng, W.; Shen, Z.; Jordan, R. F. Copolymerization of Ethylene and Vinyl Fluoride by (Phosphine-sulfonate)Pd(Me)(py) Catalysts. *J. Am. Chem. Soc.* **2007**, *129*, 15450−15451. (b) Shen, Z.; Jordan, R. F. Copolymerization of Ethylene and Vinyl Fluoride by (Phosphine-bis(arenesulfonate))PdMe(pyridine) Catalysts: Insights into Inhibition Mechanisms. *Macromolecules* **2010**, *43*, 8706−8708. (c) Liu, Q.; Jordan, R. F. Synthesis and Reactivity of Phosphine-sulfonate Palladium(II) Alkyl Complexes that Contain Methoxy Substituents. *J. Organomet. Chem.* **2019**, *896*, 207−214.

(8) (a) Boone, H. W.; Athey, P. S.; Mullins, M. J.; Philipp, D.; Muller, R.; Goddard, W. A. Copolymerization Studies of Vinyl Chloride and Vinyl Acetate with Ethylene Using a Transition-metal Catalyst. *J. Am. Chem. Soc.* **2002**, *124*, 8790−8791. (b) Stockland, R. A.; Jordan, R. F. Reaction of Vinyl Chloride with a Prototypical Metallocene Catalyst: Stoichiometric Insertion and β-Cl Elimination Reactions with *rac*-(EBI)ZrMe$^+$ and Catalytic Dechlorination/Oligomerization to Oligopropylene by *rac*-(EBI)$ZrMe_2$/MAO. *J. Am. Chem. Soc.* **2000**, *122*, 6315−6316. (c) Stockland, R. A.; Foley, S. R.; Jordan, R. F. Reaction of Vinyl Chloride with Group 4 Metal Olefin Polymerization Catalysts. *J. Am. Chem. Soc.* **2003**, *125*, 796−809. (d) Foley, S. R.; Stockland, R. A.; Shen, H.; Jordan, R. F. Reaction of Vinyl Chloride with Late Transition Metal Olefin Polymerization Catalysts. *J. Am. Chem. Soc.* **2003**, *125*, 4350−4361. (e) Leicht, H.; Göttker-Schnetmann, I.; Mecking, S. Incorporation of Vinyl Chloride in Insertion Polymerization. *Angew. Chem., Int. Ed.* **2013**, *52*, 3963−3966. (f) Kilyanek, S. M.; Stoebenau, E. J.; Vinayavekhin, N.; Jordan, R. F. Mechanism of the Reaction of Vinyl Chloride with (α-diimine)PdMe$^+$ Species. *Organometallics* **2010**, *29*, 1750−1760. (g) Philipp, D. M.; Muller, R. P.; Goddard, W. A.; Storer, J.; McAdon, M.; Mullins, M. Computational Insights on the Challenges for Polymerizing Polar Monomers. *J. Am. Chem. Soc.* **2002**, *124*, 10198−10210. (h) Strazisar, S. A.; Wolczanski, P. T. Insertion of H_2C═CHX (X = F, Cl, Br, O^{i}Pr) into (^{t}Bu_3SiO)$_3TaH_2$ and β-X-Elimination from (^{t}Bu_3SiO)$_3HTaCH_2CH_2X$ (X = OR): Relevance to Ziegler-Natta Copolymerizations. *J. Am. Chem. Soc.* **2001**, *123*, 4728−4740.

(9) The insertion of CS2 into Ir-F and Pt-F bonds has also been reported. (a) Kläring, P.; Braun, T. Insertion of CS_2 into Iridium-fluorine Bonds. *Angew. Chem., Int. Ed.* **2013**, *52*, 11096−11101. (b) Evans, J. A.; Hacker, M. J.; Kemmitt, R. D. W.; Russell, D. R.; Stocks, J. Insertion of Carbon Disulphide into a Metal−fluorine Bond: Crystal Structure of [Pt(S_2CF)(PPh_3)$_2$][HF_2]. *J. Chem. Soc., Chem. Commun.* **1972**, 72−73.

(10) (a) Fraser, S. L.; Antipin, M. Y.; Khroustalyov, V. N.; Grushin, V. V. Molecular Fluoro Palladium Complexes. *J. Am. Chem. Soc.* **1997**, *119*, 4769−4770. (b) Watson, D. A.; Su, M.; Teverovskiy, G.; Zhang, Y.; García-Fortanet, J.; Kinzel, T.; Buchwald, S. L. Formation of ArF from LPdAr(F): Catalytic Conversion of Aryl Triflates to Aryl Fluorides. *Science* **2009**, *325*, 1661−1664. (c) Pilon, M. C.; Grushin, V. V. Synthesis and Characterization of Organopalladium Complexes Containing a Fluoro Ligand. *Organometallics* **1998**, *17*, 1774−1781. (d) Grushin, V. V.; Marshall, W. J. trans-Difluoro Complexes of Palladium(II). *J. Am. Chem. Soc.* **2009**, *131*, 918−919. (e) Ball, N. D.; Kampf, J. W.; Sanford, M. S. Synthesis and Reactivity of Palladium(II) Fluoride Complexes Containing Nitrogen-donor Ligands. *Dalton Trans* **2010**, *39*, 632−640. (f) Ball, N. D.; Sanford, M. S. Synthesis and Reactivity of a Mono-sigma-aryl Palladium(IV) Fluoride Complex. *J. Am. Chem. Soc.* **2009**, *131*, 3796−3797. (g) Andrew, R. E.; Chaplin, A. B. Synthesis, Structure and Dynamics of NHC-based Palladium Macrocycles. *Dalton Trans* **2014**, *43*, 1413−1423. (h) Huacuja, R.; Herbert, D. E.; Fafard, C. M.; Ozerov, O. V. A Terminal Palladium Fluoride Complex Supported by an Anionic PNP Pincer Ligand. *J. Fluorine Chem.* **2010**, *131*, 1257−1261. (i) Martínez-Prieto, L. M.; Melero, C.; del Río, D.; Palma, P.; Cámpora, J.; Álvarez, E. Synthesis and Reactivity of Nickel and Palladium Fluoride Complexes with PCP Pincer Ligands. NMR-Based Assessment of Electron-Donating Properties of Fluoride and Other Monoanionic Ligands. *Organometallics* **2012**, *31*, 1425−1438. (j) Yandulov, D. V.; Tran, N. T. Aryl-fluoride Reductive Elimination from Pd(II): Feasibility Assessment from Theory and Experiment. *J. Am. Chem. Soc.* **2007**, *129*, 1342−1358. (k) Cairns, M. A.; Dixon, K. R.; McFarland, J. J. Fluoro-complexes of Platinum Metals. *J. Chem. Soc., Dalton Trans.* **1975**, 1159. (l) Yahav, A.; Goldberg, I.; Vigalok, A. Synthesis of the Elusive $(R_3P)_2MF_2$(M = Pd, Pt) Complexes. *J. Am. Chem. Soc.* **2003**, *125*, 13634.

(11) (a) Cattalini, L.; Martelli, M. Mechanism of Catalytic Cis-trans Isomerization of Planar Diacidodiaminopalladium(II) Complexes. *J. Am. Chem. Soc.* **1969**, *91*, 312−316. (b) Conley, M. P.; Jordan, R. F. Cis/trans Isomerization of Phosphinesulfonate Palladium(II) Complexes. *Angew. Chem., Int. Ed.* **2011**, *50*, 3744−3746. (c) Zhou, X.; Lau, K.-C.; Petro, B. J.; Jordan, R. F. *cis* /*trans* Isomerization of *o* -Phosphino-Arenesulfonate Palladium Methyl Complexes. *Organometallics* **2014**, *33*, 7209−7214.

(12) (a) Jasim, N. A.; Perutz, R. N.; Whitwood, A. C.; Braun, T.; Izundu, J.; Neumann, B.; Rothfeld, S.; Stammler, H.-G. Contrasting Reactivity of Fluoropyridines at Palladium and Platinum: C-F

DOI: 10.1021/acs.organomet.9b00545
Organometallics 2019, 38, 4250−4260

Oxidative Addition at Palladium, P-C and C-F Activation at Platinum. *Organometallics* **2004**, *23*, 6140−6149. (b) Breyer, D.; Braun, T.; Kläring, P. Synthesis and Reactivity of the Fluoro Complex *trans*-[Pd(F)(4-C_5NF_4)($Pr_2PCH_2CH_2OCH_3$)$_2$]: C−F Bond Formation and Catalytic C−F Bond Activation Reactions. *Organometallics* **2012**, *31*, 1417−1424. (c) Flemming, J. P.; Pilon, M. C.; Borbulevitch, O. Y.; Antipin, M. Y.; Grushin, V. V. The Trans Influence of F, Cl, Br and I Ligands in a Series of Square-planar Pd(II) Complexes. Relative Affinities of Halide Anions for the Metal Centre in trans-[(Ph_3P)$_2$Pd(Ph)X]. *Inorg. Chim. Acta* **1998**, *280*, 87−98. (d) Furuya, T.; Benitez, D.; Tkatchouk, E.; Strom, A. E.; Tang, P.; Goddard, W. A.; Ritter, T. Mechanism of C-F Reductive Elimination from palladium(IV) Fluorides. *J. Am. Chem. Soc.* **2010**, *132*, 3793−3807.

(13) (a) Bourgeois, C. J.; Garratt, S. A.; Hughes, R. P.; Larichev, R. B.; Smith, J. M.; Ward, A. J.; Willemsen, S.; Zhang, D.; DiPasquale, A. G.; Zakharov, L. N.; Rheingold, A. L. Synthesis and Structural Characterization of (Perfluoroalkyl)fluoroiridium(III) and (Perfluoroalkyl)methyliridium(III) Compounds. *Organometallics* **2006**, *25*, 3474. (b) Grushin, V. V. Palladium Fluoride Complexes: One More Step Toward Metal-Mediated C-F Bond Formation. *Chem. - Eur. J.* **2002**, *8*, 1006−1014.

(14) Dolbier, W. R. *Guide to Fluorine NMR for Organic Chemists*; John Wiley & Sons, Inc.: Hoboken, NJ, 2009.

(15) Allen, F. H.; Kennard, O.; Watson, D. G.; Brammer, L.; Orpen, A. G.; Taylor, R. Tables of Bond Lengths Determined by X-ray and Neutron Diffraction. Part 1. Bond Lengths in Organic Compounds. *J. Chem. Soc., Perkin Trans. 2* **1987**, *2*, S1.

(16) Gómez, M.; Rendón, N.; Álvarez, E.; Mereiter, K.; Poveda, M. L.; Paneque, M. Functionalization of 3-Iridacyclopentenes. *Chem. - Eur. J.* **2017**, *23*, 16346−16356.

(17) Holmsen, M. S. M.; Nova, A.; Balcells, D.; Langseth, E.; Øien-Ødegaard, S.; Heyn, R. H.; Tilset, M.; Laurenczy, G. trans-Mutation at Gold(III): A Mechanistic Study of a Catalytic Acetylene Functionalization via a Double Insertion Pathway. *ACS Catal.* **2017**, *7*, 5023−5034.

(18) For Other C-bound metal enolate complexes, see: (a) Fafard, C. M.; Ozerov, O. V. Retardation of *β*-hydrogen Elimination in PNP Pincer Complexes of Pd. *Inorg. Chim. Acta* **2007**, *360*, 286−292. (b) Hetterscheid, D. G. H.; Bens, M.; de Bruin, B. Ir^{II}(ethene): Metal or Carbon Radical? Part II: Oxygenation via Iridium or Direct Oxygenation at Ethene? *Dalton Trans* **2005**, 979−984. (c) Gómez, M.; Rendón, N.; Álvarez, E.; Mereiter, K.; Poveda, M. L.; Paneque, M. Functionalization of 3-Iridacyclopentenes. *Chem. - Eur. J.* **2017**, *23*, 16346−16356. (d) Murahashi, S.; Nozakura, S.; Fuji, S. Some Reactions of Mercuridiacetaldehyde. *Bull. Chem. Soc. Jpn.* **1965**, *38*, 1840−1844. (e) Krom, M.; Peters, T.; Coumans, R.; Sciarone, T.; Hoogboom, J.; terBeek, S.; Schlebos, P.; Smits, J.; de Gelder, R.; Gal, A. 3-Metalla-1,2-dioxolanes and Their Reactivity. *Eur. J. Inorg. Chem.* **2003**, *2003*, 1072.

(19) (a) Shirini, F.; Mamaghani, M.; Seddighi, M. Sulfonated Rice Husk Ash (RHA-SO3H): A Highly Powerful and Efficient Solid Acid Catalyst for the Chemoselective Preparation and Deprotection of 1,1-diacetates. *Catal. Commun.* **2013**, *36*, 31−37. (b) Deka, N.; Kalita, D. J.; Borah, R.; Sarma, J. C. Iodine as Acetylation Catalyst in the Preparation of 1,1-Diacetates from Aldehydes. *J. Org. Chem.* **1997**, *62*, 1563−1564.

(20) Evidence for both mechanisms has been reported in other studies. See ref 5 and (a) Henry, P. M. Palladium(II)-catalyzed Exchange and Isomerization Reactions. *Acc. Chem. Res.* **1973**, *6*, 16−24. (b) Zhu, G.; Lu, X. Reactivity and Stereochemistry of beta-Heteroatom Elimination. A Detailed Study through a Palladium-Catalyzed Cyclization Reaction Model. *Organometallics* **1995**, *14*, 4899−4904. (c) Peng, H.; Liu, G. Palladium-Catalyzed Tandem Fluorination and Cyclization of Enynes. *Org. Lett.* **2011**, *13*, 772.

(21) (a) Control computations show that this simple system reproduces the key features of ethylene insertion of (PO)PdR(CH_2=CH_2) complexes (R = propyl). Thus, *cis-P,R*-(PH_2O)PdR(CH_2=CH_2) is 6 kcal/mol more stable than *trans-P,Me*-(PH_2O)PdR(CH_2=CH_2), and the barrier to insertion for *cis-P,R*-(PH_2O)PdR(CH_2=CH_2) (34 kcal/mol) is higher than that for *trans-P,R*-(PH_2O)PdR(CH_2=CH_2) (13 kcal/mol). The preferred pathway for the reaction of *cis-P,R*-(PH_2O)PdR(CH_2=CH_2) is isomerization to the *trans-P,R* isomer followed by insertion. Displacement of py from (PH_2O)PdMe(py) by ethylene is modestly endergonic (*cis-P,Me* isomer: ΔG = +7 kcal/mol; *trans-P,Me* isomer: ΔG = +2). These results are in line with previous results for analogous model and real (PO)PdR catalysts. (b) Noda, S.; Nakamura, A.; Kochi, T.; Chung, L. W.; Morokuma, K.; Nozaki, K. Mechanistic Studies on the Formation of Linear Polyethylene Chain Catalyzed by Palladium Phosphine-Sulfonate Complexes: Experiment and Theoretical Studies. *J. Am. Chem. Soc.* **2009**, *131*, 14088−14100. (c) Nakano, R.; Chung, L. W.; Watanabe, Y.; Okuno, Y.; Okumura, Y.; Ito, S.; Morokuma, K.; Nozaki, K. Elucidating the Key Role of Phosphine-Sulfonate Ligands in Palladium-Catalyzed Ethylene Polymerization: Effect of Ligand Structure on the Molecular Weight and Linearity of Polyethylene. *ACS Catal.* **2016**, *6*, 6101−6113. (d) Black, R. E.; Jordan, R. F. Synthesis and Reactivity of Palladium(II) Alkyl Complexes That Contain Phosphine-Cyclopentanesulfonate Ligands. *Organometallics* **2017**, *36*, 3415−3428.

(22) Minenkov, Y.; Singstad, Å.; Occhipinti, G.; Jensen, V. R. The Accuracy of DFT-Optimized Geometries of Functional Transition Metal Compounds: A Validation Study of Catalysts for Olefin Metathesis and Other Reactions in the Homogeneous Phase. *Dalton Trans* **2012**, *41*, 5526−5541.

(23) (a) Dispersion corrections (Becke−Johnson damping) were found to not change the overall reaction profiles by more than ∼0.5 kcal/mol and were omitted. (b) Grimme, S.; Ehrlich, S.; Goerigk, L. Effect of the Damping Function in Dispersion Corrected Density Functional Theory. *J. Comput. Chem.* **2011**, *32*, 1456−1465.

(24) Tomasi, J.; Mennucci, B.; Cammi, R. Quantum Mechanical Continuum Solvation Models. *Chem. Rev.* 2005, *105*, 2999−3094 and references therein.

(25) Klamt, A.; Moya, C.; Palomar, J. A Comprehensive Comparison of the IEFPCM and SS(V)PE Continuum Solvation Methods with the COSMO Approach. *J. Chem. Theory Comput.* **2015**, *11*, 4220−4225.

(26) Solvent corrections performed using the COSMO continuum model. Klamt, A.; Schüürmann, G. COSMO: A New Approach to Dielectric Screening in Solvents with Explicit Expressions for the Screening Energy and Its Gradient. *J. Chem. Soc., Perkin Trans. 2* **1993**, *2* (5), 799−805.

(27) Solvated fluoride has been successfully treated using a variety of PCM models including COSMO. (a) Bora, S. J.; Dutta, R.; Kalita, D. J.; Chetia, B. Novel Isophthalohydrazide-CDB24C8 Cryptand Derivative for the Selective Recognition of Fluoride Ion: An Experimental and DFT Study. *Spectrochim. Acta, Part A* **2018**, *204*, 225−231. (b) Iqbal, N.; Abid Ali, S.; Munir, I.; Khan, S.; Ayub, K.; al-Rashida, M.; Islam, M.; Shafiq, Z.; Ludwig, R.; Hameed, A. Acridinedione as Selective Flouride Ion Chemosensor: A Detailed Spectroscopic and Quantum Mechanical Investigation. *RSC Adv.* **2018**, *8*, 1993−2003. (c) Bhat, H. R.; Jha, P. C. Selective Complexation of Cyanide and Fluoride Ions with Ammonium Boranes: A Theoretical Study on Sensing Mechanism Involving Intramolecular Charge Transfer and Configurational Changes. *J. Phys. Chem. A* **2017**, *121*, 3757−3767. (d) Ghosh, T.; Maiya, B. G.; Wong, M. W. Fluoride Ion Receptors Based on Dipyrrolyl Derivatives Bearing Electron-Withdrawing Groups: Synthesis, Optical and Electrochemical Sensing, and Computational Studies. *J. Phys. Chem. A* **2004**, *108*, 11249−11259.

(28) Zhao, H.; Ariafard, A.; Lin, Z. *β*-Heteroatom Versus *β*-Hydrogen Elimination: A Theoretical Study. *Organometallics* **2006**, *25*, 812.

(29) Vela, J.; Lief, G. R.; Shen, Z.; Jordan, R. F. Ethylene Polymerization by Palladium Alkyl Complexes Containing Bis(aryl)-phosphino-toluenesulfonate Ligands. *Organometallics* **2007**, *26*, 6624−6635.

DOI: 10.1021/acs.organomet.9b00545
Organometallics 2019, 38, 4250−4260

(30) (a) Christe, K. O.; Wilson, W. W. Reaction of the Fluoride Anion with Acetonitrile. Chloroform and Methylene Chloride. *J. Fluorine Chem.* **1990**, *47*, 117−120. (b) Christe, K. O.; Wilson, W. W. Nuclear Magnetic Resonance Spectrum of the Fluoride Anion. *J. Fluorine Chem.* **1990**, *46*, 339−342.
(31) (a) Gel'mbol'dt, V. O.; Ennan, A. A. Pentacoordinate Fluorosilicate Anions. *Russ. Chem. Rev.* **1989**, *58*, 371−380. (b) Pevec, A.; Demšar, A. The Variations in Hydrogen Bonding in Hexafluorosilicate Salts of Protonated Methyl Substituted Pyridines and Tetramethylethylenediamine. *J. Fluorine Chem.* **2008**, *129*, 707−712. (c) Conley, B. D.; Yearwood, B. C.; Parkin, S.; Atwood, D. A. Ammonium Hexafluorosilicate Salts. *J. Fluorine Chem.* **2002**, *115*, 155−160. (d) Nahra, F.; Brill, M.; Gómez-Herrera, A.; Cazin, C. S. J.; Nolan, S. P. Transition Metal Bifluorides. *Coord. Chem. Rev.* **2016**, *307*, 65−80.

DOI: 10.1021/acs.organomet.9b00545
Organometallics 2019, 38, 4250−4260